

Document downloaded from:

<http://hdl.handle.net/10251/162577>

This paper must be cited as:

Gonzalez-Camejo, J.; Robles Martínez, Á.; Seco, A.; Ferrer, J.; Ruano, MV. (2020). On-line monitoring of photosynthetic activity based on pH data to assess microalgae cultivation. *Journal of Environmental Management*. 276:1-8.
<https://doi.org/10.1016/j.jenvman.2020.111343>



The final publication is available at

<https://doi.org/10.1016/j.jenvman.2020.111343>

Copyright Elsevier

Additional Information

1 **On-line monitoring of photosynthetic activity based on pH data to assess**
2 **microalgae cultivation**

3 J. González-Camejo^{1*}, A. Robles¹, A. Seco¹, J. Ferrer², M.V. Ruano¹

4 ¹CALAGUA – Unidad Mixta UV-UPV, Departament d'Enginyeria Química,
5 Universitat de València, Avinguda de la Universitat s/n, 46100 Burjassot, Valencia,
6 Spain.

7 ²CALAGUA – Unidad Mixta UV-UPV, Institut Universitari d'Investigació
8 d'Enginyeria de l'Aigua i Medi Ambient – IIAMA, Universitat Politècnica de València,
9 Camí de Vera s/n, 46022 Valencia, Spain

10 *Corresponding autor: J. González-Camejo (josue.gonzalez@uv.es)

11

12 **Abstract**

13 Microalgae performance of outdoor cultivation systems is influenced by environmental
14 and operating dynamics. Monitoring and control systems are needed to maximise
15 biomass productivity and nutrient recovery. The goal of this work was to corroborate
16 that pH data could be used to monitor microalgae performance by means of data from
17 an outdoor membrane photobioreactor (MPBR) plant. In this system, microalgae
18 photosynthetic activity was favoured over other physical and biological processes, so
19 that the pH data dynamics was theoretically related to the microalgae carbon uptake rate
20 (CUR).

21 Short- and long-term continuous operations were tested to corroborate the relationship
22 between the first derivate of pH data dynamics (pH') and microalgae photosynthetic
23 activity. Short-term operations showed a good correlation between gross pH' values and
24 MPBR performance. An indicator of the maximum daily average microalgae activity
25 was assessed by a combination of on-line pH' measurements obtained in the long-term

26 and a microalgae growth kinetic model. Both indicators contributed to the development
27 of advanced real-time monitoring and control systems to optimise microalgae
28 cultivation technology.

29

30 **1. Introduction**

31 Microalgae cultivation has been receiving increasing interest from the scientific
32 community since it allows nutrient recovery, CO₂ biofixation and valorisation of the
33 algal biomass produced (Guldhe et al., 2017). However, industrial microalgae
34 cultivation plants are still scarce, mainly due to their low efficiency which increases
35 operating costs (Acién et al., 2018).

36 Improving the microalgae activity in photobioreactors (PBRs) and open ponds is likely
37 to be a way of reducing these high costs (Salama et al., 2017). In this respect, some
38 authors have evaluated indirect measurements to analyse the microalgae photosynthetic
39 activity. By way of example, Perin et al. (2016) measured the chlorophyll fluorescence
40 *in vivo* of *Nannochloropsis gaditana*. Romero-Villegas et al. (2018) used the maximum
41 quantum yield (F_v/F_m) to indirectly measure the photosynthetic activity; while Rossi et
42 al. (2018) used standardised respirometric assays to evaluate microalgae and bacteria
43 activity simultaneously. However, these off-line methods require a certain delay and
44 cannot be monitored in real-time.

45 Microalgae activity can also be assessed by key performance indicators such as
46 microalgae biomass productivity and nutrient recovery rates (González-Camejo et al.,
47 2020a; Marazzi et al., 2019), for which suspended solids and nutrient concentrations
48 must be measured. Although on-line probes and analysers can monitor ammonium,
49 nitrate, and suspended solids concentrations, they usually have high capital and
50 maintenance costs and are not always as reliable as expected (Havlik et al., 2013). For

51 this reason, they are often measured by time-consuming and expensive laboratory
52 analyses (Foladori et al., 2018). Other parameters like pH, light and temperature are also
53 highly related to microalgae growth (Abu-Ghosh et al., 2020; Robles et al., 2020).
54 These variables are commonly measured by on-line sensors, which are reliable and
55 involve lower costs (Ruano et al., 2009). Developing on-line monitoring strategies
56 based on dynamic modelling of data obtained by cost-effective sensors would thus be of
57 great interest. Some authors have made advances in this research field; for instance,
58 Pawlowski et al. (2019) described a model-based control to regulate pH in raceway
59 ponds; Robles et al. (2020) used pH and dissolved oxygen on-line sensors to describe
60 the performance of a raceway pond during the start-up phase; De-Luca et al. (2018)
61 proposed two optimisation approaches to prevent critical conditions caused by using
62 inaccurate weather forecast; while Foladori et al. (2018) evaluated the nutrient removal
63 of a microalgae-bacteria culture for lab-scale wastewater treatment by using pH, oxygen
64 and oxidation-reduction potential sensors. However, long-term full-scale data to apply
65 on-line monitoring strategies are still needed to make microalgae cultivation systems
66 more efficient.

67 An approach based on pH data to on-line monitor microalgae photosynthetic activity in
68 a membrane photobioreactor (MPBR) fed by sewage coming from an anaerobic
69 membrane bioreactor (AnMBR) is proposed in this work. An indicator of instantaneous
70 microalgae activity was obtained from these on-line pH measurements which could be
71 used as an input for real-time short-term control. An indicator of the maximum
72 microalgae activity was assessed by a combination of these on-line pH measurements
73 and a microalgae growth kinetic model which provided the long-term monitoring and
74 control of microalgae performance. These indicators would rapidly help to detect
75 significant variations in the microalgae cultivation system.

76

77 **2. Material and Methods**

78 *2.1. Membrane photobioreactor plant*

79 The MPBR plant was operated outdoors in Valencia (Spain). Two methacrylate PBRs
80 were connected to a membrane tank (MT) which allowed solids (SRT) and hydraulic
81 retention time (HRT) to be decoupled. Two different systems were used: i) one
82 containing 550-L PBRs (25-cm wide); and ii) another equipped with 230-L PBRs (10-
83 cm wide).

84 The oxygen concentration in each PBR was always above saturation due to their
85 continuous aeration system and the microalgae activity. Pure CO₂ (99.9%) was
86 introduced into this system when the pH was over a set value of 7.5 to maintain it
87 within a controlled range (i.e. 7.0-7.5). Adding CO₂ also avoided carbon limitation and
88 limited phosphorus precipitation and ammonia volatilisation (Iasimone et al., 2018).
89 White LED lamps (Unique IP65, 40w) supplied a continuous irradiance of 300 μmol·m⁻²·s⁻¹
90 on the back surface of each PBR.

91 The following on-line sensors were used to monitor the outdoor MPBR plant: i) one
92 pH-temperature sensor (pHDsc DPD1R1, Hach Lange) and ii) one dissolved oxygen
93 (LDOsc LXV416.99.20001, Hach Lange) sensor in each PBR; and iii) one sensor to
94 measure the photosynthetically active radiation (PAR) on the PBR surface (Apogee
95 Quantum SQ-200). To maintain the accuracy of the pH and oxygen sensors, they were
96 calibrated every two weeks. In addition, the buffer and the salt bridge were replaced
97 once a year. To perform process control and data acquisition, the sensors were
98 connected to a PLC controlled by a SCADA system, which was fully described by
99 Viruela et al. (2018).

100

101 *2.1.2. Wastewater medium and microalgae*

102 Microalgae were originally collected from the walls of the clarifiers of an urban WWTP
103 as explained in González-Camejo et al. (2020b). They were cultivated using the effluent
104 of an AnMBR plant (Durán et al., 2020), which nutrient concentrations are shown in
105 Table A.1.

106 Green microalgae *Chlorella* and *Scenedesmus* were the main microorganisms of the
107 culture according to microscopic observations. Variations in the culture strain
108 composition were not considered to involve significant changes in MPBR performance
109 (González-Camejo et al., 2019; 2020a; Sutherland et al., 2020). The inoculum also
110 contained heterotrophic and nitrifying bacteria in negligible concentrations.

111

112 *2.1.3. Operating conditions*

113 Short- and long-term MPBR performance were evaluated with the goal of correlating
114 pH data with instantaneous and daily average microalgae photosynthetic activity,
115 respectively. Short-term continuous operation was assessed in the 10-cm MPBR plant
116 for six days (SRT = 4.5 d; HRT = 1.25 d). The MPBR plant was operated long-term
117 continuously from June 2015 to November 2017. In the 25-cm-wide MPBR plant, the
118 HRT varied from 1 to 3.5 d, while SRT changed from 4.5 to 9 d. In the 10-cm-wide
119 MPBR plant, HRT and SRT from 1 to 1.5 d and 2 to 4.5 d, respectively (Table A.2).

120 All the periods shown in Table A.2 began with a start-up stage which is described in
121 González-Camejo et al. (2019). Periods used for maintenance labours and start-up
122 stages were not considered in this long-term evaluation.

123 *2.2. Analytical methods*

124 Standard Methods (APHA, 2012) was followed to measure ammonium (4500-NH₃-G),
125 phosphate (4500-P-F), nitrite (4500-NO₂-B) and nitrate (4500-NO₃-H) concentrations.

126 To this aim, Smartchem 200 (Westco Scientific Instruments) was used. Volatile
127 suspended solids (VSS) concentration of the MPBR was analysed by method 2540-E
128 (APHA, 2012). Optical density of 680 nm (OD) was obtained using a fluorometer
129 (AquaPen-C AP-C 100). Six respirometric tests which followed the protocol of Rossi et
130 al. (2018), were done in a period of two weeks to assess the microalgae and nitrifying
131 bacteria activity simultaneously.

132

133 *2.3. pH monitoring*

134 The pH control (see Section 2.1) was turned off each day for 30 minutes at midnight
135 while keeping the constant artificial light supplied by the lamps (Section 2.1). Due to
136 variations in the equilibrium of inorganic carbon species (Foladori et al., 2018), during
137 this non-pH-controlled periods a lineal increase in pH values was observed (Figure
138 A.1). The first derivative of this pH data dynamics (pH') was used as an on-line
139 monitoring parameter and depended on several factors:

- 140 ▪ Microalgae photosynthetic activity (main factor), which in turn depends on other
141 factors such as light irradiance, biomass concentration and pigment content
142 amongst others (Fernández et al., 2016; Wagner et al., 2018). Theoretically, the
143 faster the metabolic activity of microalgae, the faster inorganic carbon is consumed
144 and the higher the pH' (Eze et al., 2018; Robles et al., 2020).
- 145 ▪ CO_2 stripping, which is related to the mass transfer efficiency, which in turn
146 depends on bubble size, air flow rate, culture height, and pH set-point. All these
147 parameters remained constant during MPBR operations, except for the air flow rate,
148 which varied with the PBR light path (Table A.2).
- 149 ▪ Temperature, which affects CO_2 stripping due to variations in CO_2 solubility in
150 water. This variation was considered negligible since CO_2 solubility in the MPBR

151 plant (temperatures around 20-30 °C) only varied in the range of 0.13-0.17% (Perry
152 et al., 1997). The PBRs were also closed to the atmosphere, which reduces CO₂
153 stripping.

154 ■ CO₂ production by heterotrophic bacteria. This was considered negligible due to the
155 low BOD₅ entering the MPBR (11-13 mgO₂·L⁻¹), which favoured microalgae
156 autotrophic growth (Rossi et al., 2020). In fact, microalgae biomass concentration
157 was found to be directly related to microalgae cell concentration in the evaluated
158 system (González-Camejo et al., 2020a), suggesting that microalgae were the
159 predominant organism in the culture.

160 ■ Nitrifying bacteria activity, which affects pH since nitrification reduces the culture
161 alkalinity (Foladori et al., 2018). However, nitrification was not considered relevant
162 during the experimental period as the sum of nitrite and nitrate concentrations, which
163 can be used as an indirect measure of nitrification rate (González-Camejo et al.,
164 2020c) remained at concentrations lower than 10 mgN·L⁻¹. This was also
165 corroborated by six respirometric tests (according to the protocol of Rossi et al.
166 (2018)), in which oxygen uptake rate (OUR) of the nitrifying bacteria only reached
167 an average of 4.4% of the oxygen production rate (OPR) of microalgae (Figure
168 A.2).

169 ■ CO₂ production by microalgae respiration. However, microalgae respiration rate is
170 usually associated with microalgae activity (Rossi et al., 2018). Indeed, the
171 respirometric tests showed that the OUR due to microalgae respiration accounted
172 for an average of 11% of the net microalgae OPR (p-value < 0.05; R² = 0.672; n =
173 6). Microalgae respiration was therefore not considered to significantly influence
174 pH' variation dynamics through the experimental period.

175 Summarising, microalgae activity was considered as the only factor related to carbon
176 concentration variations which had a significant influence on pH dynamics in the
177 MPBR plant. pH' was thus theoretically related to the microalgae carbon uptake rate
178 (CUR) in the evaluated system (Eq. 1).

$$179 \text{CUR} \approx -\alpha_1 \cdot \text{pH}' \quad (\text{Eq. 1})$$

180 Where CUR ($\text{mgC} \cdot \text{L}^{-1} \cdot \text{d}^{-1}$) is the carbon uptake rate, pH' is the first derivative from pH
181 data dynamics ($\text{pHunit} \cdot \text{d}^{-1}$), and α_1 is a distributed factor.

182 pH' could be therefore assessed as an on-line measurement of the daily average
183 microalgae CUR, which is in turn related to microalgae photosynthetic activity. It is
184 important to note that if microalgae CUR is assessed from pH data in other cultivation
185 system where factors different than photosynthetic activity are neither negligible nor
186 constant, an adjustment in the model would be required.

187

188 2.3.1. Short-term pH monitoring

189 During the short-term period, the culture pH varied freely (no CO_2 addition, Section 2.1)
190 for 10 minutes each hour of the day to measure pH' . These pH' calculations were used
191 as an on-line indicator of the instantaneous microalgae activity under the system's
192 specific operating and environmental conditions.

193

194 2.3.2. Microalgae growth kinetic model

195 An indicator of the daily maximum microalgae activity was assessed using a model
196 based on the pH' calculations and previous results on microalgae activity modelling
197 (Robles et al, 2020). As already mentioned, pH variations were mainly related to
198 microalgae CUR in the evaluated system. Since CUR is usually related to the average
199 light irradiance (I_{av}) by a hyperbolic function (Fernández et al., 2016; Tripathi and

200 Kumar, 2017), Eq. (2) was used to determine pH' as a function of I_{av} when considering
201 constant respiration conditions, no nutrient limitation and non-inhibiting dissolved
202 oxygen and pH conditions:

$$203 \quad pH' = pH'_{max} \cdot I_i + \alpha_2 \quad (\text{Eq. 2})$$

204 Where pH'_{max} is the maximum pH' ($pH \cdot \text{unit} \cdot d^{-1}$), I_i ($i=1:3$) is a given function related to
205 the average light irradiance (I_{av}), and α_2 is a distributed factor.

206 Eq. (2) is only valid under non-nutrient-limiting conditions. For this, pH' values
207 obtained under limiting nitrogen concentrations; i.e. under $10 \text{ mgN} \cdot \text{L}^{-1}$ (González-
208 Camejo et al., 2019), were discarded.

209 Three different normalising factors related to I_{av} ($\mu\text{mol} \cdot \text{m}^{-2} \cdot \text{s}^{-1}$) (I_1 , I_2 , and I_3) were
210 tested. I_1 (Eq. 3) is analogous to the duty cycle (Robles et al., 2020), which is defined as
211 the proportional time which microalgae receive light (Fernández-Sevilla et al., 2018). I_2
212 (Eq. 4) corresponds to a Monod-type factor in which I_{av} is analogous to the substrate
213 and PAR serve as “semisaturation constant” (Martínez et al., 2019). Lastly, I_3 is
214 modified Monod-type factor obtained from Fernández et al. (2016) (Eq. 5).

$$215 \quad I_1 = \frac{I_{av}}{PAR} \quad (\text{Eq. 3})$$

$$216 \quad I_2 = \frac{I_{av}}{I_{av} + PAR} \quad (\text{Eq. 4})$$

$$217 \quad I_3 = \frac{I_{av}^n}{k_i \cdot e^{m \cdot I_{av}} + I_{av}^n} \quad (\text{Eq. 5})$$

218 where PAR ($\mu\text{mol} \cdot \text{m}^{-2} \cdot \text{s}^{-1}$) corresponds to the total photosynthetically active radiation
219 received by the PBR (i.e. solar light and irradiance from LED lamps), while n (1.045),
220 m (0.0021) and k_i ($174 \mu\text{mol} \cdot \text{m}^{-2} \cdot \text{s}^{-1}$) are form parameters reported by Fernández et al.
221 (2016). The I_{av} was calculated with the equations reported by González-Camejo et al.
222 (2020a).

223

224 2.3.3. Normalised pH' and microalgae performance indicators

225 Based on the above-mentioned kinetics, the relationships between factors derived from
226 pH' and performance indicators derived from biomass productivity (BP), N-recovery
227 rate (NRR) and P-recovery rate (PRR) were assessed. For this, pH', BP, NRR and PRR
228 were normalised by either one or two factors related to microalgae activity: i.e. I_i (I_1 , I_2
229 or I_3), PAR, solar PAR (sPAR), OD or VSS. All the normalised parameters used for the
230 long-term data evaluation are shown in Table A.3.

231

232 2.4. Statistical analysis

233 To assess the long-term data ($n = 170$), the Partial Least Squares (PLS) algorithm was
234 applied. pH' and its normalised parameters were used as predictors (X), while MPBR
235 performance indicators and their normalised parameters were selected as responses (Y)
236 (Table A.3). PLS was carried out by using the mix Omics library through R-software
237 (version 3.2.3).

238 Long-term data were scaled to unit variance (and mean-centred) to equalise the weight
239 of the variables in the PLS models (González-Camejo et al., 2020a).

240

241 3. Results and discussion

242 3.1. Short-term pH data

243 The main results from this short-term period are shown in Table 1. pH' generally
244 increased during daytime hours due to the rising solar PAR, usually reaching the
245 maximum daily values around noon (Figure 1). An exception to the habitual behaviour
246 was observed on day 2, when pH' was higher in the early morning (low solar PAR) than
247 at midday (maximum solar PAR) (Figure 1). This was probably due to the reduced
248 microalgae activity from day 1 to day 2, when both biomass productivity and NRR

249 significantly fell (Table 1). It should be noted that pH' values in darkness were quite
250 high: 15-40 $\text{pHunits}\cdot\text{d}^{-1}$ (Figure 1) for two reasons: i) the PBRs were lit by an additional
251 source of artificial light (Section 2.1), and ii) carbon absorption of microalgae takes
252 place in the photosynthesis dark reactions, i.e. there is no need for light irradiance to
253 modify the pH (Manhaeghe et al., 2019).

254 The highest pH' values, i.e. 35-45 $\text{pHunit}\cdot\text{d}^{-1}$ (Figure 1) occurred at the beginning of the
255 short-term operations. Since the short-term period was preceded by a start-up phase
256 (González-Camejo et al., 2019), microalgae were expected to be more active at this
257 point. The MPBR plant thus showed the highest NRR ($26.3\text{ mgN}\cdot\text{L}^{-1}\cdot\text{d}^{-1}$) and biomass
258 productivity ($284\text{ mgVSS}\cdot\text{L}^{-1}\cdot\text{d}^{-1}$) on day 1.

259 However, from midday of day 2 until the beginning of day 5 (hour 110), pH' remained
260 at low values in the range of 17-23 $\text{pHunit}\cdot\text{d}^{-1}$ (Figure 1). This trend was corroborated
261 by reduced biomass productivity from 170 to 139 $\text{mgVSS}\cdot\text{L}^{-1}\cdot\text{d}^{-1}$ in days 2-5; while
262 NRR fell from 22.9 to 16.4 $\text{mgN}\cdot\text{L}^{-1}\cdot\text{d}^{-1}$ in the same period. Later, pH' rose again, but
263 not as much as at the beginning, i.e. values of 25-33 $\text{pHunit}\cdot\text{d}^{-1}$ during hours 110-140
264 (Figure 1). In this case microalgae performance slightly increased: from 16.4 $\text{mgN}\cdot\text{L}^{-1}\cdot\text{d}^{-1}$
265 in day 5 to 18.1 $\text{mgN}\cdot\text{L}^{-1}\cdot\text{d}^{-1}$ in day 6 for NRR and from 139 $\text{mgVSS}\cdot\text{L}^{-1}\cdot\text{d}^{-1}$ to 148
266 $\text{mgVSS}\cdot\text{L}^{-1}\cdot\text{d}^{-1}$ for biomass productivity in the same period. NRR and biomass
267 productivity therefore seemed to be directly related to gross pH' values (and hence to
268 gross CUR) in the short term, showing a good correlation, i.e. R^2 of 0.895 and 0.820 (n
269 = 4) for NRR and BP, respectively. Gross pH' can thus be a good indicator of punctual
270 microalgae photosynthetic activity in this system. pH' would hence allow on-line
271 monitoring of microalgae performance at any time of the cultivation process.

272 Regarding PRR, it followed a different trend than biomass productivity and NRR (Table
273 1). It is possible that phosphorus luxury uptake (Solovchenko et al., 2019) and/or

274 phosphorus precipitation would have had a significant influence on this short-term
275 assessment. In fact, in this period hydroxyapatite (HAP) and octacalcium phosphate
276 (OCP) were oversaturated (Table A.4 and A.5), which made them likely to precipitate.
277 Phosphorus uptake was therefore not directly related to the photosynthetic activity in
278 the short term.

279

280 *3.2. Long-term validation of pH data*

281 *3.2.1. MPBR performance*

282 The MPBR plant functionally operated under variable ambient and operating conditions
283 (see Table A.2) for 310 days in the 25-cm MPBR plant and 225 days in the 10-cm
284 MPBR plant. To assess the performance of each MPBR plant, NRR, PRR and biomass
285 productivity were used. In the 25-cm MPBR plant, nutrient recovery rates (Figure 2a)
286 varied in the range of 4-15 $\text{mgN}\cdot\text{L}^{-1}\cdot\text{d}^{-1}$ and 0.2-2 $\text{mgP}\cdot\text{L}^{-1}\cdot\text{d}^{-1}$, while productivity
287 (Figure 2b) was around 40-115 $\text{mgVSS}\cdot\text{L}^{-1}\cdot\text{d}^{-1}$. In the 10-cm MPBR plant, those
288 parameters rose to 10-35 $\text{mgN}\cdot\text{L}^{-1}\cdot\text{d}^{-1}$, 0.8-5 $\text{mgP}\cdot\text{L}^{-1}\cdot\text{d}^{-1}$ and 110-300 $\text{mgVSS}\cdot\text{L}^{-1}\cdot\text{d}^{-1}$,
289 respectively (Figure 2c;2d). The 10-cm plant thus showed significantly better results
290 than the 25-cm plant. Further information about differences in MPBR performance of
291 these systems can be found in González-Camejo et al. (2020c).

292 It must be highlighted that the theoretical correlation between the evolution of pH' and
293 performance indicators during continuous operation is hardly observed in Figure 2,
294 probably because there were other factors that could have affected it. For this reason,
295 the correlation between pH' measurements with the performance indicators needs to be
296 corroborated by statistical analyses such as PLS (see Sections 3.2.2 and 3.3).

297

298 3.2.2. Screening and classification of pH data

299 A preliminary PLS analysis was performed to corroborate the use of pH' as on-line
300 microalgae CUR measurement as predicted in Eq. (1). The pH' values and pH'
301 normalised by light and/or biomass concentration were used as predictors. The
302 analogous normalised parameters of NRR, PRR and BP were employed as responses
303 (Table A.3). This preliminary PLS analysis (data not shown) allowed for the screening
304 of the following variables:

- 305 ▪ Parameters normalised by OD and VSS were closely related in all cases, which
306 agrees with previous results that reported high correlation between these parameters
307 (González-Camejo et al., 2020a;2020c). The parameters normalised by VSS were
308 thus discarded and those normalised by OD were selected for further evaluation.
309 OD was the preferred option since it is related to the chlorophyll content of
310 microalgae (González-Camejo et al., 2020a; Markou et al., 2017). However, VSS
311 considers other microorganisms' biomass, not only microalgae (Di Caprio, 2020).
312 In addition, OD can be monitored on-line (Havlik et al., 2013; Lucker et al., 2014)
313 but VSS is usually obtained off-line (APHA, 2012).
- 314 ▪ Parameters normalised by I_1 and I_2 gave similar results, obtaining a slight better
315 correlation with I_2 . In this respect, de Farias Silva et al. (2020) reported that the
316 Monod model can be applied when no more than a limiting substrate is used. In this
317 study, only light was considered a limiting factor (see Section 2.3.2). I_2 was thus
318 selected for further assessment while I_1 was discarded.
- 319 ▪ As the PBRs were supplied with constant artificial light, PAR and sPAR presented
320 similar variability. For this, only the parameters normalised by PAR were
321 considered for further evaluation.

322 After this screening, a single PLS model was created using all the data ($n = 170$) from
323 both MPBR plants (10-cm and 25-cm plants). Three principal components (PCs)
324 accounted for the cumulative explained variance of 90.8%, which were from PC1
325 (37.2%), PC2 (35.0%) and PC3 (18.6%). Figure 3a and 3b show that pH' is
326 significantly correlated to MPBR performance in terms of NRR, PRR and BP, since
327 these indicators are close together in the plot. Gross pH' was thus confirmed as a valid
328 parameter to monitor MPBR performance. It should be noted that the pH' parameters
329 normalised by I_i , PAR and OD also showed a good correlation with their associated
330 normalised performance indicators. The PLS results thus corroborate pH' being a good
331 parameter for on-line monitoring the long-term MPBR operation under variable
332 environmental and operating conditions.

333 It should be noted that two discernible groups of data were found in both the X and Y
334 blocks (Figure 3c and 3d) from both plants: 25-cm (samples 1-88, blue numbers) and
335 10-cm MPBR plant (samples 88-170, orange numbers). These results confirmed their
336 different performance regarding the parameters analysed in the model. Indeed, Figure 2
337 shows different pH' ranges for both MPBR systems, i.e. 4-18 $\text{pHunit}\cdot\text{d}^{-1}$ and 8-25
338 $\text{pHunit}\cdot\text{d}^{-1}$ for 25-cm and 10-cm MPBR plant, respectively. Apart from the different
339 microalgae performance obtained in both systems (as previously reported in González-
340 Camejo et al. (2020c)), these differences in pH' values could also have been influenced
341 by the different air flow rate supplied to the PBRs (Table A.2). For this, analysing the
342 data obtained from each plant separately would better assess the potential of pH' data
343 for monitoring their performance.

344

345 3.2.3. pH data evaluation and validation

346 According to the data screening explained in Section 3.2.2, pH', pH':OD, pH':PAR,
347 pH':I₂, pH':I₃, pH':PAR:OD, pH':I₂:OD and pH':I₃:OD were used as predictors (X) in
348 the following PLS analyses, while analogous normalised parameters related to NRR,
349 PRR and biomass productivity were used in the Y-axis. Two additional PLS analyses
350 were carried out: one for data from the 25-cm plant (n = 88) and another for the 10-cm
351 plant (n = 82). For the 10-cm plant, three PCs accounted for 98.7% of the cumulative
352 explained variance for PC1 (45.4%), PC2 (30.4%) and PC3 (22.9%). For the 25-cm
353 plant, three PCs attained 99.1% of the cumulative explained variance, in which PC1,
354 PC2 and PC3 accounted for 65.2%, 24.2% and 9.7%, respectively.

355 As can be seen in Figure 4, in both plants normalised pH' parameters showed better
356 correlation with their normalised performance indicators than the non-normalised
357 parameters as they are generally closer in the plots. These results therefore suggest that
358 normalising pH', BP, NRR and PRR to monitor maximum daily average microalgae
359 activity can provide more reliable results to evaluate these microalgae cultivation
360 systems than non-normalised factors. It should be remembered that the correlation
361 between the normalised pH' predictors and normalised PRR responses was usually less
362 significant than the correlation with the normalised NRR and biomass productivity
363 responses (Figure 4) probably influenced by phosphorus uptake being dependent on the
364 intracellular phosphorus concentration (Solovchenko et al., 2019) and the possibility of
365 phosphorus precipitation by means of HAP and OCP (Table A.4 and A.5) (not
366 considered in this study).

367 The PLS model for the 10-cm MPBR plant showed in general closer correlations
368 between normalised pH' and performance indicators than the 25-cm plant (Figure 4). It
369 must be considered that there were some experimental periods operated at long SRT in

370 the latter plant during which grazers and other organisms proliferated (González-
371 Camejo et al., 2019). This varied the relationship between OD and VSS (Figure A.3)
372 and could probably have had an influence on the relationship among the parameters
373 evaluated.

374 It should also be noted that the closest correlations were obtained with the parameters
375 normalised by I_2 or I_3 (which depend on I_{av}), although this correlation was similar to
376 those between parameters normalised by I_2 and OD or by I_3 and OD (Figure 4). On the
377 other hand, the parameters normalised by PAR displayed less significant correlations in
378 both plants (Figure 4). This was probably due to light attenuation within the culture.
379 Light transmittance is exponentially reduced along the PBR mainly due to the light
380 absorbed by the photosynthetic microalgae pigments (Wagner et al., 2018).
381 Consequently, the same PAR on the PBR surface can supply significantly different I_{av}
382 values according to the culture characteristics (González-Camejo et al., 2020c; Romero-
383 Villegas et al., 2018). I_{av} thus appears as a relevant factor in the model. On the other
384 hand, normalising by OD showed a good correlation between the parameters analysed
385 but did not improve the correlation between parameters in comparison to I_2 and I_3 . This
386 was probably because OD is closely related to I_{av} (Barbera et al., 2020).

387 The parameters normalised by I_2 showed a slightly better correlation than those
388 normalised by I_3 in the 10-cm plant (Figure 4a and 4b). However, the correlation
389 between parameters normalised by I_2 in the 25-cm plant was quite similar to the
390 correlation between parameters normalised by I_3 (Figure 4c and 4d). It should be
391 considered that the I_3 factor was obtained from a dynamic model used for raceway
392 reactors (Fernández et al., 2016) which depths are usually around 15-45 cm (Arbib et
393 al., 2017) unlike flat-panel PBRs, which usually present light paths of around 1-10 cm
394 (Slegers et al., 2011). This model was thus likely to fit the 25-cm plant better than the

395 10-cm plant. To sum up, the results obtained in this study suggest that pH' values can
396 be used to monitor the maximum carbon assimilation capacity of microalgae in
397 continuous long-term MPBR operations.

398

399 **4. Conclusions**

400 pH data were used to on-line monitor microalgae photosynthetic activity in an MPBR
401 system. Short-term operations showed a relationship between on-line pH' values and
402 MPBR performance in terms of NRR and BP. Gross pH' measurements were therefore
403 identified as indicators of the microalgae photosynthetic activity dynamics throughout
404 the day. Long-term operations showed a relationship between on-line pH'
405 measurements and microalgae performance indicators (i.e. BP, NRR and PRR), all of
406 them normalised by considering a microalgae growth kinetic model. pH' was therefore
407 also identified as an indicator of daily maximum microalgae activity. This pH'
408 parameter could hence be used in advanced real-time monitoring and control strategies
409 for MPBR optimisation.

410

411 **Acknowledgments**

412 Authors would like to acknowledge the Ministry of Economy and Competitiveness
413 (Spain) for their support in Projects CTM2014-54980-C2-1-R and CTM2014-54980-
414 C2-2-R, together with the European Regional Development Fund. The author J.
415 González-Camejo would also like to thank the Ministry of Education, Culture and Sport
416 (Spain) for its support (pre-doctoral fellowship, FPU14/05082).

417

418 **E-supplementary data can be found in on-line version of the manuscript.**

419

420 **References**

- 421 1. Abu-Ghosh, S., Dubinsky, Z., Iluz, D., 2020. Acclimation of thermotolerant
422 algae to light and temperature interaction. *J. Phycol.* 56, 662-670.
423 <https://doi.org/10.1111/jpy.12964>
- 424 2. Ación Fernández, F.G., Gómez-Serrano, C., Fernández-Sevilla, J.M., 2018.
425 Recovery of Nutrients From Wastewaters Using Microalgae. *Frontiers in*
426 *Sustainable Food Systems*, 2(59). <http://dx.doi.org/10.3389/fsufs.2018.00059>
- 427 3. APHA, 2012. Standard methods for the examination of water and wastewater,
428 22nd. American Public Health Association, American Water Works Association,
429 Water Environment Federation, Washington, USA.
- 430 4. Arbib, Z., de Godos, I., Ruiz, J., Perales, J.A., 2017. Optimization of pilot high
431 rate algal ponds for simultaneous nutrient removal and lipids production. *Sci.*
432 *Total Environ.* 589, 66–72. <http://dx.doi.org/10.1016/j.scitotenv.2017.02.206>
- 433 5. Barbera, E., Sforza, E., Grandi, A., Bertucco, A., 2020. Uncoupling solid and
434 hydraulic retention time in photobioreactors for microalgae mass production: A
435 model-based analysis. *Chem. Eng. Sci.* 218, 115578.
436 <https://doi.org/10.1016/j.ces.2020.115578>
- 437 6. de Farias Silva, C.E., de Oliveira Cerqueira, R.B., de Lima Neto, C.F., de
438 Andrade, F.P., de Oliveira Carvalho, F., Tonholo, J., 2020. Developing a kinetic
439 model to describe wastewater treatment by microalgae based on simultaneous
440 carbon, nitrogen and phosphorous removal. *J. Environ. Chem. Eng.* 8(3),
441 103792. <https://doi.org/10.1016/j.jece.2020.103792>
- 442 7. De-Luca, R., Trabuio, M., Barolo, M., Bezzo, F., 2018. Microalgae growth
443 optimization in open ponds with uncertain weather data. *Comput. Chem. Eng.*
444 117, 410–419. <https://doi.org/10.1016/j.compchemeng.2018.07.005>

- 445 8. Di Caprio, F., 2020. Methods to quantify biological contaminants in microalgae
446 cultures. *Algal Res* 49, 101943. <https://doi.org/10.1016/j.algal.2020.101943>
- 447 9. Durán, F., Robles, A., Giménez, J.B., Ferrer, J., Ribes, J., Serralta, J., 2020.
448 Modeling the anaerobic treatment of sulfate-rich urban wastewater: Application
449 to AnMBR technology. *Water Res.* 184, 116133.
450 <https://doi.org/10.1016/j.watres.2020.116133>
- 451 10. Eze, V.C, Velasquez-Orta, S.B., Hernández-García, A., Monje-Ramírez, I.,
452 Orta-Ledesma, M.T., 2018. Kinetic modelling of microalgae cultivation for
453 wastewater treatment and carbon dioxide sequestration. *Algal Res.* 32, 131–141.
454 <https://doi.org/10.1016/j.algal.2018.03.015>
- 455 11. Fernández, I., Acién, F.G., Guzmán, J.L., Berenguel, M., Mendoza, J.L., 2016.
456 Dynamic model of an industrial raceway reactor for microalgae production.
457 *Algal Res.* 17, 67-78. <http://dx.doi.org/10.1016/j.algal.2016.04.021>
- 458 12. Fernández-Sevilla, J.M., Brindley, C., Jiménez-Ruíz, N., Acién, F.G., 2018. A
459 simple equation to quantify the effect of frequency of light/dark cycles on the
460 photosynthetic response of microalgae under intermittent light. *Algal Res.* 35,
461 479–487. <https://doi.org/10.1016/j.algal.2018.09.026>
- 462 13. Foladori, P., Petrini, S., Andreottola, G., 2018. Evolution of real municipal
463 wastewater treatment in photobioreactors and microalgae-bacteria consortia
464 using real-time parameters. *Chem. Eng. J.* 345, 507–516.
465 <https://doi.org/10.1016/j.cej.2018.03.178>
- 466 14. González-Camejo, J., Barat, R., Aguado, D., Ferrer, J., 2020a. Continuous 3-
467 year outdoor operation of a flat-panel membrane photobioreactor to treat effluent
468 from an anaerobic membrane bioreactor. *Water Res.* 169, 115238.
469 <https://doi.org/10.1016/j.watres.2019.115238>

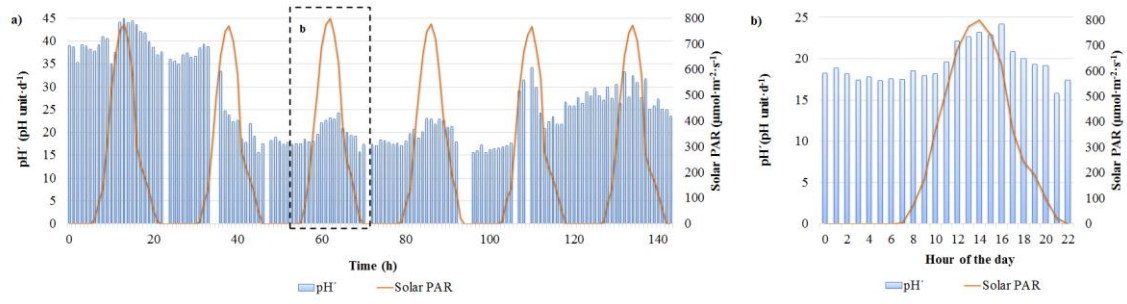
- 470 15. González-Camejo, J., Pachés, M., Marín, A., Jiménez-Benítez, A., Seco, A.,
471 Barat, R., 2020b. Production of microalgal external organic matter in
472 a *Chlorella*-dominated culture: influence of temperature and stress factors.
473 *Environ. Sci.: Water Res. Technol.* 6. 1828-1841.
474 <https://doi.org/10.1039/D0EW00176G>
- 475 16. González-Camejo, J., Aparicio, S., Jiménez-Benítez, A., Pachés, M., Ruano,
476 M.V., Borrás, L., Barat, R., Seco, A., 2020c. Improving membrane
477 photobioreactor performance by reducing light path: operating conditions and
478 key performance indicators. *Water Res.* 172, 115518.
479 <https://doi.org/10.1016/j.watres.2020.115518>
- 480 17. González-Camejo, J., Jiménez-Benítez, A., Ruano, M.V., Robles, A., Barat, R.,
481 Ferrer, F., 2019. Optimising an outdoor membrane photobioreactor for tertiary
482 sewage treatment. *J. Environ. Manag.* 245, 76-85.
483 <https://doi.org/10.1016/j.jenvman.2019.05.010>
- 484 18. Guldhe, A., Kumari, S., Ramanna, L., Ramsundar, P., Singh, P., Rawat, I., Bux,
485 F., 2017. Prospects, recent advancements and challenges of different wastewater
486 streams for microalgal cultivation. *J. Environ. Manag.* 203, 299-315.
487 <http://dx.doi.org/10.1016/j.jenvman.2017.08.012>
- 488 19. Havlik, I., Lindner, P., Scheper, T., Reardon, K.F., 2013. On-line monitoring of
489 large cultivations of microalgae and cyanobacteria. *Trends Biotechnol.* 31, 406–
490 414. <https://doi.org/10.1016/j.tibtech.2013.04.005>.
- 491 20. Iasimone, F., Panico, A., De Felice, V., Fantasma, F., Iorizzi, M., Pirozzi, F.,
492 2018. Effect of light intensity and nutrients supply on microalgae cultivated in
493 urban wastewater: Biomass production, lipids accumulation and settleability

- 494 characteristics. J. Environ. Manag. 223, 1078–1085.
495 <https://doi.org/10.1016/j.jenvman.2018.07.024>
- 496 21. Lucker, B.F., Hall, C.C., Zegarac, R., Kramer, D.M., 2014. The environmental
497 photobioreactor (ePBR): An algal culturing platform for simulating dynamic
498 natural environments. Algal Res. 6, 242–249.
499 <http://dx.doi.org/10.1016/j.algal.2013.12.007>
- 500 22. Manhaeghe, D., Michels, S., Rousseau, D.P.L., Van Hulle, S.W.H., 2019. A
501 semi-mechanistic model describing the influence of light and temperature on the
502 respiration and photosynthetic growth of *Chlorella vulgaris*. Bioresour. Technol.
503 274, 361-370. <https://doi.org/10.1016/j.biortech.2018.11.097>
- 504 23. Marazzi, F., Bellucci, M., Rossi, S., Fornaroli, R., Ficara, E., Mezzanotte, V.,
505 2019. Outdoor pilot trial integrating a sidestream microalgae process for the
506 treatment of centrate under non optimal climate conditions. Algal Res. 39,
507 101430. <https://doi.org/10.1016/j.algal.2019.101430>
- 508 24. Markou, G., Dao, L.H.T., Muylaert, K., Beardall, J., 2017. Influence of different
509 degrees of N limitation on photosystem II performance and heterogeneity of
510 *Chlorella vulgaris*. Algal Res. 26, 84-92.
511 <http://dx.doi.org/10.1016/j.algal.2017.07.005>
- 512 25. Martínez, C., Mairet, F., Martinon, P., Bernard, O., 2019. Dynamics and control
513 of a periodically forced microalgae culture. IFAC Papers OnLine 52(1) 922-927.
514 <https://doi.org/10.1016/j.ifacol.2019.06.180>
- 515 26. Pawlowski, A., Guzmán, J.L., Berenguel, M., Ación, F.G., 2019. Control System
516 for pH in Raceway Photobioreactors Based on Wiener Models. IFAC-Papers
517 OnLine 52-1, 928–933. <https://doi.org/10.1016/j.ifacol.2019.06.181>

- 518 27. Perin, G., Cimetta, E., Monetti, F., Morosinotto, T., Bezzo, F., 2016. Novel
519 micro-photobioreactor design and monitoring method for assessing microalgae
520 response to light intensity. *Algal Res.* 19, 69–76.
- 521 28. Perry, R.H., Green, D.W., Maloney, J.O., 1997. Perry's chemical
522 engineers' handbook-7th Ed. McGraw-Hill. United States of America. ISBN 0-
523 07-049841-5.
- 524 29. Robles, A., Capson-Tojo, G., Galés, A., Ruano, M.V., Sialve, B., Ferrer, J.,
525 Steyer, J.P., 2020. Microalgae-bacteria consortia in high-rate ponds for treating
526 urban wastewater: elucidating the key state indicators during the start-up period.
527 *J. Environ. Manag.* 261, 110244. <https://doi.org/10.1016/j.jenvman.2020.110244>
- 528 30. Romero-Villegas, G.I., Fiamengo, M., Ación-Fernández, F.G., Molina-Grima,
529 E., 2018. Utilization of centrate for the outdoor production of marine microalgae
530 at the pilot-scale in raceway photobioreactors. *J. Environ. Manag.* 228, 506–516.
531 <https://doi.org/10.1016/j.jenvman.2018.08.020>
- 532 31. Rossi, S., Casagli, F., Mantovani, M., Mezzanotte, V., Ficara, E., 2020.
533 Selection of photosynthesis and respiration models to assess the effect of
534 environmental conditions on mixed microalgae consortia grown on wastewater.
535 *Bioresour. Technol.* 305, 122995.
536 <https://doi.org/10.1016/j.biortech.2020.122995>
- 537 32. Rossi, S., Bellucci, M., Marazzi, F., Mezzanotte, V., Ficara, E., 2018. Activity
538 assessment of microalgal-bacterial consortia based on respirometric tests. *Water*
539 *Sci Technol.* 78(1-2), 207-215. <https://doi.org/10.2166/wst.2018.078>
- 540 33. Ruano, M.V., Ribes, J., Seco, A., Ferrer, J., 2009. Low cost-sensors as a real
541 alternative to on-line nitrogen analysers in continuous systems. *Wat. Sci. Tech.*
542 60(12), 3261-3268. <http://dx.doi.org/10.2166/wst.2009.607>

- 543 34. Salama, E.S., Jeon, B.H., Chang, S.W., Lee, S.h., Roh, H.-S., Yang, I.S.,
544 Kurade, M.B., El-Dalatony, M.M., Kim, D.-H., Kim, K.H., Kim, S., 2017.
545 Interactive effect of indole-3-acetic acid and diethyl aminoethyl hexanoate on
546 the growth and fatty acid content of some microalgae for biodiesel production. *J.*
547 *Clean. Prod.* 168, 1017-1024. <https://doi.org/10.1016/j.rser.2017.05.091>
- 548 35. Slegers, P.M., Wijffels, R.H., van Straten, G., and van Boxtel, A.J.B., 2011.
549 Design scenarios for flat panel photobioreactors. *Appl. Energ.* 88(10), 3342-
550 3353. <https://doi.org/10.1016/j.apenergy.2010.12.037>
- 551 36. Solovchenko, A., Khozin-Goldberg, I., Selyakh, I., Semenova, L., Ismagulova,
552 T., Lukyanov, A., Mamedov, I., Vinogradova, E., Karpova, O., Konyukhov, I.,
553 Vasilieva, S., Mojzes, P., Dijkema, C., Vecherskaya, M., Zvyagin, I., Nedbal,
554 L., Gorelov, O., 2019. Phosphorus starvation and luxury uptake in green
555 microalgae revisited. *Algal Res.* 43, 101651.
556 <https://doi.org/10.1016/j.algal.2019.101651>
- 557 37. Sutherland, D.L., Park, J., Ralph, P.J., Craggs, R.J., 2020. Improved microalgal
558 productivity and nutrient removal through operating wastewater high rate algal
559 ponds in series. *Algal Res.* 47, 101850.
560 <https://doi.org/10.1016/j.algal.2020.101850>
- 561 38. Tripathi, B.N., Kumar, D., 2017. *Prospects and Challenges in Algal*
562 *Biotechnology*. Springer Science and Business Media LLC. Singapore. ISBN
563 978-981-10-1949-4
- 564 39. Viruela, A., Robles, A., Durán, F., Ruano, M.V., Barat, R., Ferrer, J., Seco, A.,
565 2018. Performance of an outdoor membrane photobioreactor for resource
566 recovery from anaerobically treated sewage. *J. Clean. Prod.* 178, 665-674.
567 <https://doi.org/10.1016/j.jclepro.2017.12.223>

568 40. Wagner, D.S., Valverde-Perez, B., Plosz, B.G., 2018. Light attenuation in
569 photobioreactors and algal pigmentation under different growth conditions –
570 Model identification and complexity assessment, *Algal Res.* 35, 488-499.
571 <https://doi.org/10.1016/j.algal.2018.08.019>
572

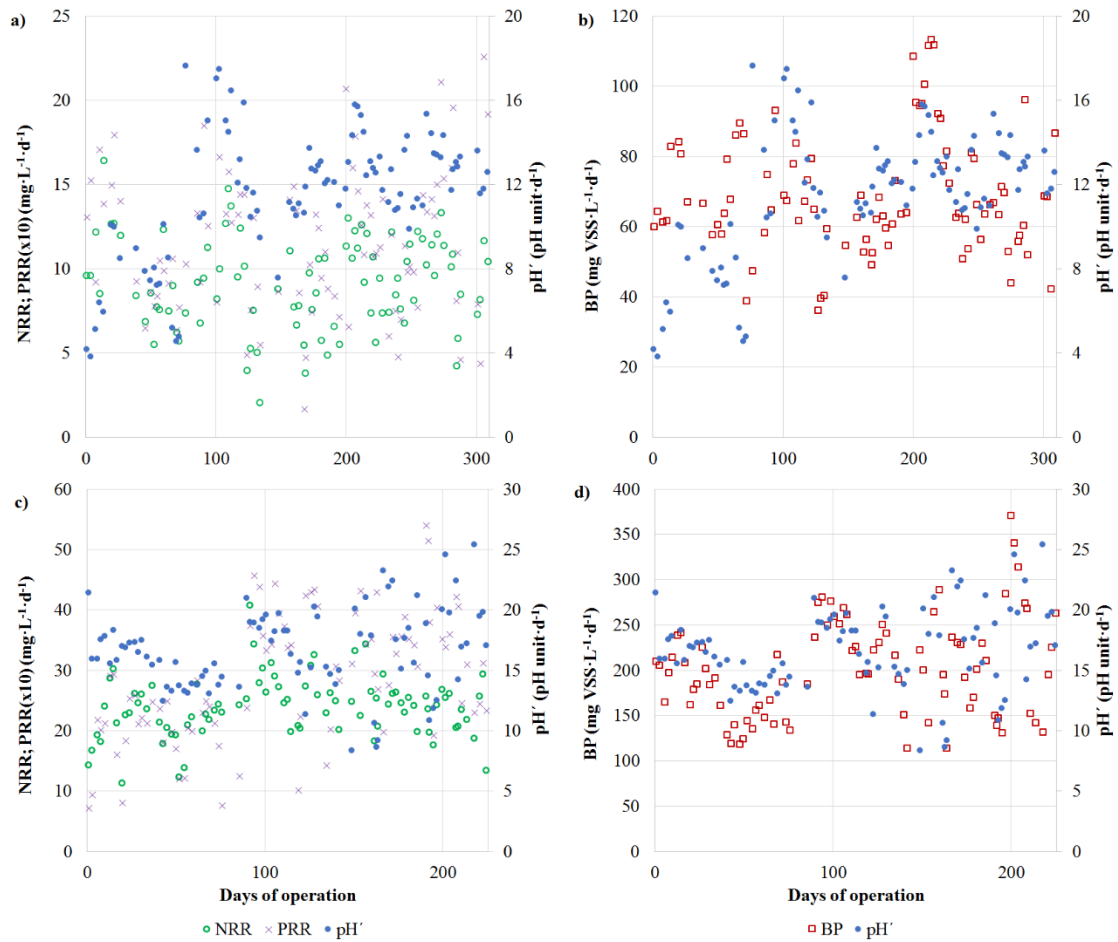


573

574 *Figure 1. Evolution of the first derivate of pH dynamics (pH') and solar PAR during: a)*

575 *6 days of continuous short-term operation; b) day 3.*

576



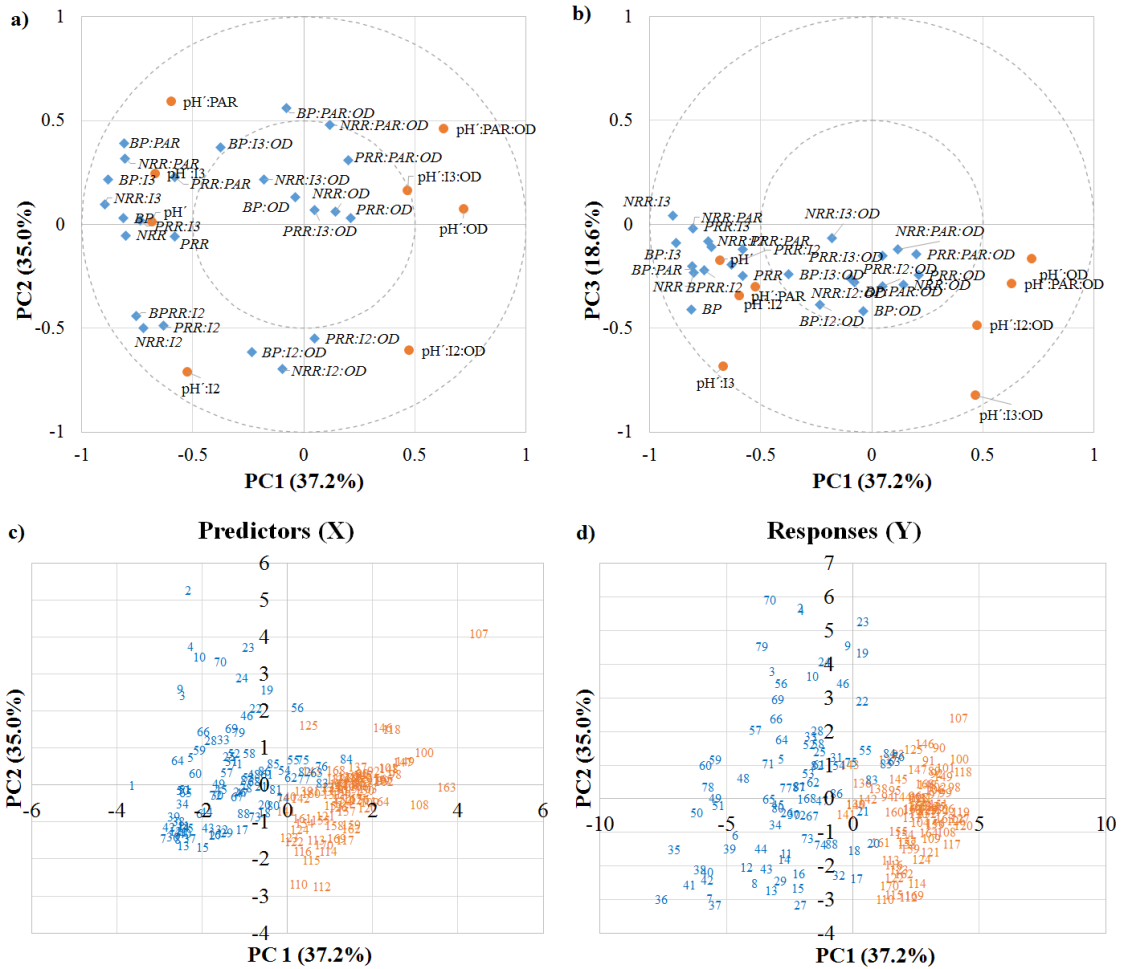
577

578 *Figure 2. Evolution during continuous operation of the 25-cm MPBR plant of: a) pH',*

579 *NRR and PRR; b) pH' and biomass productivity; evolution during continuous operation*

580 *of the 10-cm MPBR plant of: c) pH', NRR and PRR; d) pH' and biomass productivity.*

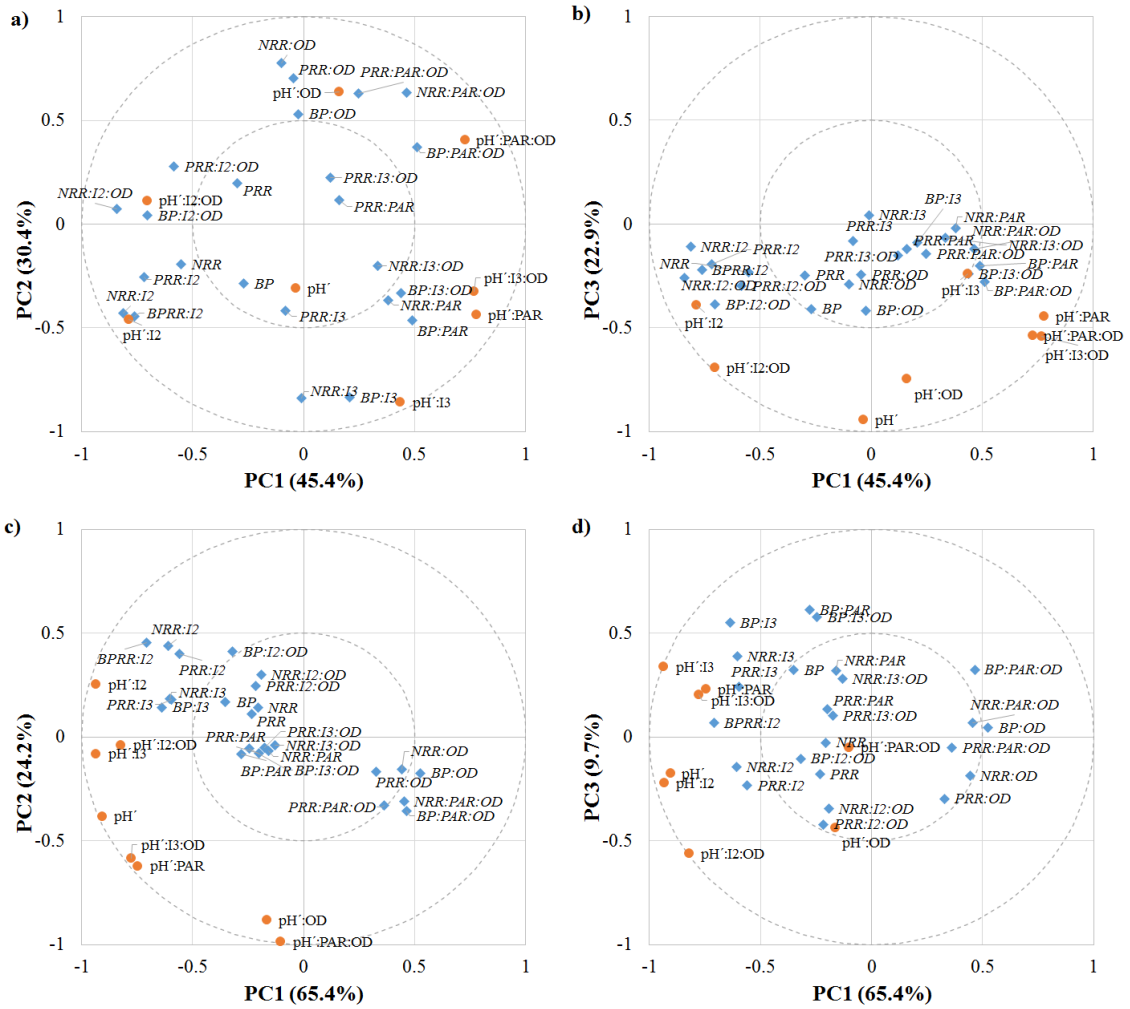
581



582

583 *Figure 3: Results of the PLS analysis (n = 170). Correlation circle plots from the*
 584 *integration of the selected predictors (pH' and normalised predictors); and responses*
 585 *(NRR, PRR, BP and their normalised parameters): a) PC-1 and PC-2; b) PC-1 and PC-*
 586 *3; score plot of the preliminary PLS model: c) Predictors (X) and d) Responses (Y).*
 587 *Blue numbers (1-88): 25-cm MPBR plant; Orange numbers (89-170) 10-cm MPBR*
 588 *plant.*

589



590

591 *Figure 4. PLS analyses. Correlation circle plots from the integration of the selected*
 592 *predictors (pH' and normalise predictors); and responses (NRR, PRR, BP and their*
 593 *normalised parameters): a and b) 10-cm MPBR plant (n = 82); c and d) 25-cm MPBR*
 594 *plant (n = 88).*

595

Table 1. Mean values of the short-term operation of the MPBR plant

Day	Solar PAR ($\mu\text{mol}\cdot\text{m}^{-2}\cdot\text{s}^{-1}$)	pH' (pH unit $\cdot\text{d}^{-1}$)	BP (mg VSS $\cdot\text{L}^{-1}\cdot\text{d}^{-1}$)	NRR (mg N $\cdot\text{L}^{-1}\cdot\text{d}^{-1}$)	PRR (mg P $\cdot\text{L}^{-1}\cdot\text{d}^{-1}$)
1	227 \pm 279	39.8 \pm 2.9	284	26.3	2.0
2	237 \pm 278	39.9 \pm 8.7	170	22.9	2.5
3	214 \pm 294	29.0 \pm 2.3	-	-	-
4	238 \pm 283	19.3 \pm 2.2	-	-	-
5	232 \pm 276	19.6 \pm 2.8	138	16.4	3.3
6	223 \pm 278	21.7 \pm 2.5	148	18.1	2.9

597 PAR: photosynthetically active radiation; pH': first derivative from pH data dynamics; BP: biomass
 598 productivity; NRR: nitrogen recovery rate; PRR: phosphorus recovery rate.